

Growth and morphology transitions in anisotropic disordered media

Belita Koiller

Instituto de Física, Universidade Federal do Rio de Janeiro, Caixa Postal 68.528, 21941-972 Rio de Janeiro, RJ, Brazil

Mark O. Robbins

Department of Physics and Astronomy, The Johns Hopkins University, 3400 N. Charles Street, Baltimore, Maryland 21218, USA

(Received 3 May 2010; published 19 August 2010)

Depinning transitions of an interface between two magnetic domains are studied within the random-field Ising model in three dimensions. The fields are uniformly distributed with width 2Δ in units of the exchange coupling. The morphology of the interface at the depinning transition varies with Δ . Self-similar morphologies characteristic of percolation are observed at large disorder, and self-affine interfaces with roughness exponent $2/3$ are formed at intermediate disorder. The multicritical point at the self-similar to self-affine transition is analyzed through finite-size scaling. The critical disorder Δ_c is substantially higher than previous estimates and lies near a local maximum in the depinning field $H_c(\Delta)$. The scaling exponent for the correlation length near Δ_c is consistent with results for a Gaussian distribution of random fields, suggesting that the form of the distribution does not change the universality class. However there is another transition to faceted growth at small disorder that is not present for Gaussian distributions. The critical field for faceted growth depends on orientation and boundary conditions. There is a unique “hard” growth direction, (001), for periodic boundary conditions, whose H_c is larger than that for all other orientations. For the more physical case of free boundary conditions, growth leads to facets with this hard orientation. This inhibits further growth and increases H_c with respect to the value for periodic boundary conditions.

DOI: [10.1103/PhysRevB.82.064202](https://doi.org/10.1103/PhysRevB.82.064202)

PACS number(s): 75.60.Ch, 68.35.Ct, 68.35.Rh, 75.60.Ej

I. INTRODUCTION

Interface motion in disordered media is an important topic in condensed-matter physics, not only because of its applications in a variety of natural systems but also because of its role in motivating the development of concepts and tools for understanding the interplay between interface morphology, critical phenomena, and phase transitions.^{1–21} Among the models explored, perhaps the simplest is the random-field Ising model (RFIM). It is able to capture the competition between an external force that drives the interface, the local disorder that aids or hinders advance of each region along the interface, and the elastic coupling between neighboring regions of the interface. In addition, unlike many other interface models,^{5–11,22} there is no explicit breaking of symmetry along a growth direction and this leads to a richer variety of growth morphologies.^{17–21}

Two classes of RFIM spin-flip models have been studied. The first allows spins to flip at any location and was designed to model Barkhausen noise in magnetic systems.^{4,14–16} The magnetization curves in this model show an ordinary critical transition at a critical strength of the disorder. The second, front-propagation class focuses on motion of an existing interface, and only allows spins adjacent to the interface to flip.^{17–21} This constraint was motivated by applications to fluid invasion of porous media,^{23,24} where fluid must flow through a connected path to invade new regions, and is implicit in most models of interface motion.^{5–12} Recent work suggests that Barkhausen noise in many systems is described by motion of existing interfaces and that long-range demagnetizing fields may play an important role in the dynamics.^{13,25}

The front propagation model leads to a greater variety of critical behavior. There are critical transitions between differ-

ent types of growth morphology as the strength of disorder varies. In addition, for any degree of disorder, there is critical behavior at the onset of steady interface growth that is characteristic of self-organized critical systems.^{1,2,26} Previous studies have examined the influence of lattice type, dimension and the distribution of disorder.^{17–21} The richest phase diagram is found for bounded distributions of disorder, where the growth morphology changes from self-similar to self-affine to faceted with decreasing disorder. Faceted growth reflects the underlying lattice anisotropy and is suppressed by unbounded (e.g., Gaussian) disorder^{17,27} or amorphous disorder in the location of spins. It may be important for many crystalline systems but bounded distributions of disorder have not been addressed in most previous studies. One interesting consequence of bounded disorder is that it can prevent flipping of spins that are not adjacent to the interface, suppressing the distinction between the classes of growth model described above. Recent studies that allowed flipping at all locations found that uniform, bounded distributions gave very different critical behavior than other distributions of random fields.¹⁶

In this paper, we present a detailed analysis of interface depinning and morphology in a three-dimensional (3D) RFIM on a simple cubic lattice.^{20,21} Growth from an initial interface is driven by an external field at zero temperature. The random fields are uniformly distributed between $\pm\Delta$. For each Δ , we identify the critical field H_c that leads to steady advance of the interface and study the interface morphology at the critical field (Fig. 1).

At large Δ , growth is completely isotropic and interfaces have a self-similar structure characteristic of percolation. At a critical disorder Δ_c , there is a transition to self-affine growth, where the advancing interface has long-range orientational order. In contrast to other growth models,^{5,9} the

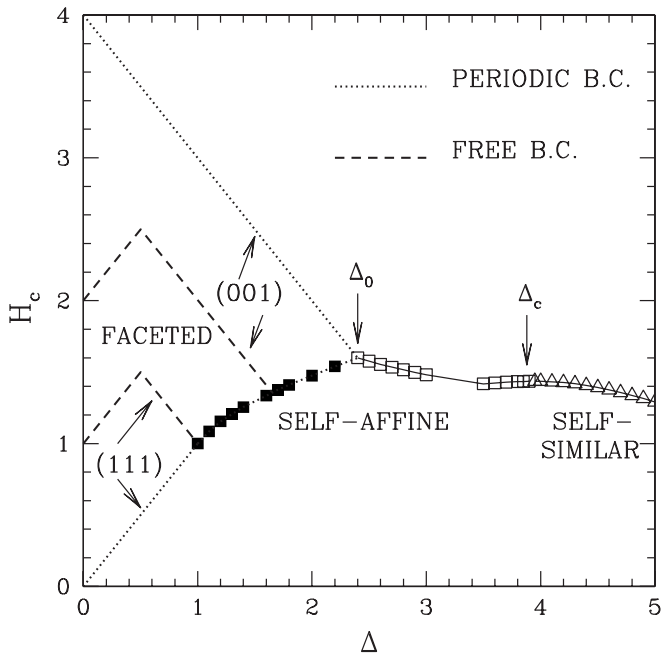


FIG. 1. Phase diagram giving the critical field H_c versus disorder Δ as a function of boundary conditions and initial interface orientation. As the disorder increases, the morphology of the interface changes from faceted (straight broken lines) to self-affine (squares) to self-similar (triangles). The self-affine to self-similar transition occurs at $\Delta_c = 3.88 \pm 0.03$, and appears to correspond to a local maximum in H_c . The faceted to self-affine transition is affected by geometry. Error bars on H_c are less than 0.1%.

value of H_c in the self-affine regime is independent of interface orientation relative to the lattice and insensitive to boundary conditions. The value of Δ_c is determined from finite-size scaling studies of the external interface,²⁷ and is significantly shifted from earlier studies.²⁰ This shift is due to the presence of regions of unflipped spins behind the moving interface, which do not arise in models with explicitly broken symmetry.⁵⁻¹¹ The critical exponent ν describing the change in correlation length with Δ appears to be the same as for unbounded distributions,²⁷ suggesting that the distribution of random fields does not change the universality class. Allowing spins to flip away from the interface does change the scaling exponents.¹⁴⁻¹⁶

At even smaller disorder, $\Delta < \Delta_0$, the anisotropy of the lattice becomes important. The critical field and growth morphology depend on growth direction and boundary conditions. In contrast to models where the growth depends explicitly on the angle relative to the local interface orientation,^{5,9} the critical field does not vary continuously with orientation. Instead, there is a unique “hard” growth orientation with a high H_c for $1 < \Delta < \Delta_0$. All other orientations have the same H_c and self-affine scaling exponent when periodic boundary conditions are applied. The finite boundaries of physically realizable systems have a strong effect on growth at all system sizes. They facilitate growth along the hard orientation while hindering it in the easiest direction. The interface tends to form facets along the hard orientation that remain pinned until the H_c for this orientation.

In Sec. II, we describe the growth model. Section III presents a comprehensive phase diagram and then discusses

finite-size scaling at the self-similar to self-affine transition, the transition to faceted growth, and the morphology of growth in systems with free boundaries. Concluding remarks are presented in Sec. IV.

II. GROWTH MODEL

As in previous studies,²⁷ we consider a zero-temperature growth algorithm for a spin system with Hamiltonian,

$$\mathcal{H} = - \sum_{\langle i,j \rangle} s_i s_j - \sum_i (\eta_i + H) s_i. \quad (1)$$

Each Ising spin ($s_i = \pm 1$) is on a site of a simple cubic lattice and is ferromagnetically coupled to its six nearest neighbors. The exchange coupling is taken as the unit of energy, and the lattice parameter as the unit of length. All spins also interact with an external magnetic field H and with local random fields η_i that are uniformly distributed: $-\Delta \leq \eta_i \leq \Delta$. Disorder is thus quantified by the parameter Δ .

All spins on the lattice are initially antiparallel to the external field, $s_i = -1$, except for those in a bottom layer where $s_i = +1$. The motion of the interface between $+1$ and -1 spins is then followed at fixed external field. Growth proceeds through single-spin flips, and only spins at the interface and antiparallel to the external field are allowed to flip (from $s_i = -1$ to $s_i = +1$). A spin flip is implemented if and only if it lowers the total energy, which corresponds to a zero-temperature simulation. Note that it is never energetically favorable for spins that are not on the interface to flip for $H < 6 - \Delta$. Thus restricting spin flips to the interface does not affect growth over the range of Δ of interest here. The situation is very different for unbounded disorder, like the Gaussian random fields considered earlier.^{14,15,27}

We varied the boundary conditions of the simulation cell and the initial orientation of the interface relative to the crystalline axes to determine their influence on interface growth. For large Δ , the results are independent of orientation and boundaries. In this limit, we present results for cubic simulation cells of side L varying between 48 and 1536. The initial domain wall is parallel to a (001) cubic crystal plane and periodic boundary conditions are imposed in this plane. As Δ decreases, lattice anisotropy and boundary conditions become important. We considered periodic systems with initial interfaces parallel to (10 λ) planes of varying λ . The initial interface was a rectangle with L spins along the x axis. We also considered initial interfaces parallel to (111) planes. Here the periodic cell was a diamond with L spins along each edge. To model finite samples, we removed the spins around the edges of the above cells. We discuss “free” boundary conditions where the distribution of random fields on surface sites is unchanged, and cases where the random fields on boundary spins are set to facilitate ($\eta_i = +\Delta$) or hinder ($\eta_i = -\Delta$) growth.

Spins are flipped until all interface spins are stable or the domain wall reaches the top of the cell. The probability that the interface will reach the top of the cell grows with increasing H . In the limit of infinite system size, the interface will reach the top of the cell if and only if the external field is larger than a critical value $H_c(\Delta)$. In finite systems, there is a

range of H near $H_c(\Delta)$ where the probability of reaching the top P increases rapidly from zero to unity. For each system size L , we studied interfaces at a value of $H_c(\Delta, L)$ where P was about 0.6.²⁸ Finite-size scaling²⁷ can be used to determine precise values of H_c in the limit $L \rightarrow \infty$ but for the largest system sizes studied here $H_c(\Delta, L)$ is always within 0.1% of the limiting value and usually an order of magnitude closer.

III. RESULTS

Figure 1 summarizes our results for the critical field H_c as a function of disorder Δ and geometry. The interface morphology observed at H_c is indicated in each case. For large Δ , H_c is independent of geometry and growth is isotropic at large scales. Our values in this regime (open symbols) are consistent with previous work by Ji and Robbins.²⁰ However, we find that the transition from self-similar to self-affine morphologies occurs at $\Delta_c = 3.88 \pm 0.03$ rather than their value of 3.41. This transition is described in detail in Sec. III A.

As Δ decreases, lattice anisotropy becomes more important. At small enough Δ , there is a faceted regime where pinned states at H_c form facets with specific lattice orientations. The faceted regime only occurs for $\Delta < \Delta_0 \approx 2.42$ (called Δ_1^c in Ref. 20) but the location of the transition to faceted growth and the value of H_c depend on orientation and boundary conditions.^{18–21} The upper dotted line for (001) interfaces with periodic boundary conditions is consistent with Ref. 20. The closed squares and lower dotted line agree with studies of (111) surfaces with periodic boundary conditions in Ref. 21. Periodic boundary conditions are hard to realize in experiments and the dashed lines show that H_c shifts dramatically when samples have free boundaries. Section III B discusses the role of lattice anisotropy at low disorder.

A. Self-similar to self-affine transition

In the high-disorder limit, the Hamiltonian is dominated by the second term in Eq. (1). Growth follows a path of “easy-to-flip” sites, i.e., spins with local fields η_i near $+\Delta$. The resulting flipped domain is a self-similar fractal in the same universality class as percolation clusters.²⁰ As Δ decreases, the exchange term in H becomes more important, producing correlations in the flipping of neighboring spins. Interface motion is correlated over a length ξ that diverges at a multicritical point^{20,24,29} $[\Delta_c, H_c(\Delta_c)]$ as $\xi \sim (\Delta - \Delta_c)^{-\nu}$, where ν is a critical exponent. Below Δ_c , the interface has a well-defined average orientation and obeys self-affine fractal scaling.² The length ξ is related to the correlation length studied in RFIM models where noninterface spins are allowed to flip. There are other, unrelated correlation lengths and exponents that describe the diverging size of “avalanches” as $H \rightarrow H_c$ for each value of Δ .^{24,29} These have been determined in previous studies of the RFIM (Ref. 20) and other front propagation models.^{4,6–12}

In previous work,^{20,24,29} a simple geometrical measure was used to quantify the range of correlations in the self-

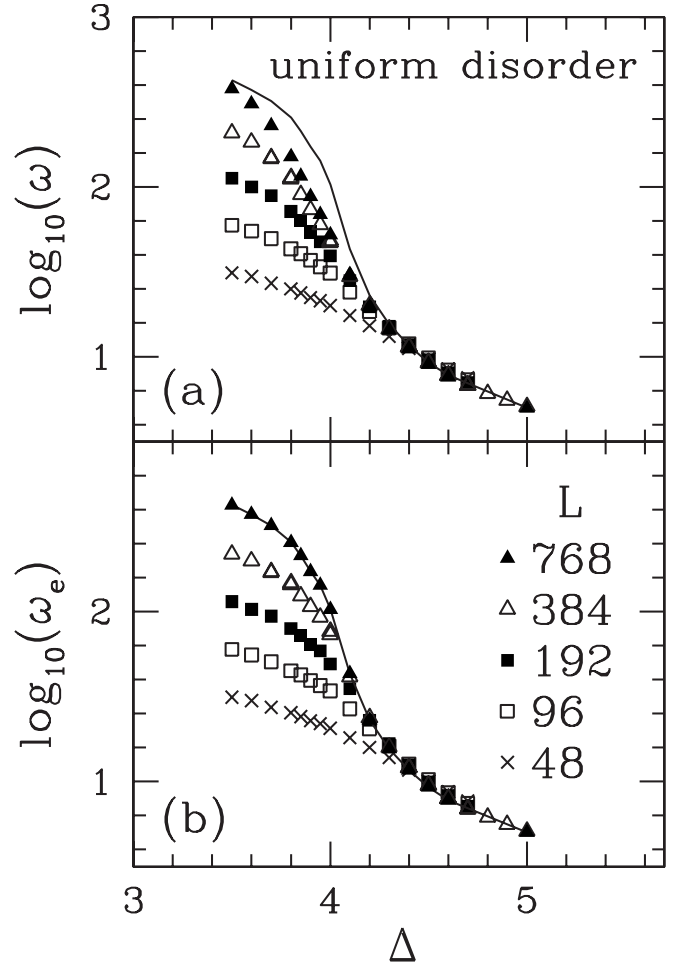


FIG. 2. (a) Finger width versus disorder Δ for the indicated simulation cell sizes. The solid line gives the external finger width (w_e) for the largest cell ($L=768$). (b) External finger widths versus disorder. In both panels, the finger widths were calculated in the plane normal to the nominal growth direction z . Statistical errors are smaller than the symbol size.

similar regime. An average finger width w was defined as the mean length of contiguous lines of $s=+1$ spins along the (100) or (010) directions. This quantity increased rapidly with decreasing disorder, and Δ_c and ν were determined^{20,24,29} from a finite-size scaling analysis that assumed w scaled with ξ . Recent studies of larger systems with Gaussian disorder²⁷ showed that w does not diverge at Δ_c and identified more accurate ways of determining Δ_c . We repeat this analysis for the case of uniform disorder in this section.

Our results for the average finger width obtained for simulation cell sizes from $L=48$ to 768 are indicated by the data points in Fig. 2(a). Finite-size scaling collapses of w do not yield good fits for any values of ν and Δ_c because the rise of w does not sharpen rapidly enough as L increases. Moreover, analysis of the domain of flipped spins shows that it is not self-similar at length scales larger than w for $\Delta \leq 4$. These observations imply that w does not diverge with ξ at Δ_c . The reason²⁷ is that the interface surrounds and leaves behind domains of unflipped ($s_i=-1$) spins. Most front

propagation models do not allow the interface height to be multivalued^{6–12} but this ability for RFIM interfaces to pass around strongly pinned spins has a dramatic effect on values of H_c and critical scaling.²⁷ Trapped domains prevent w from diverging but have no effect on the subsequent motion of the interface or the scaling behavior of the flipped region. The range of L in Ref. 20 was not large enough to detect this difficulty or to determine Δ_c with an uncertainty of less than about 0.5. Indeed, the value of $\Delta_c=3.41$ was estimated²⁰ from the location of a transition in growth mechanisms based on an analogous transition in two-dimensional (2D) systems.¹⁸ A more accurate determination of Δ_c requires a different approach.

Following Ref. 27 we define an external finger width w_e that only reflects the structure of the external interface obtained by removing all surrounded unflipped domains. The solid line in Fig. 2(a) shows w_e for $L=768$. It is close to w for large disorder but rises much more rapidly as Δ decreases. Figure 2(b) shows w_e for the same range of L shown in (a). From these data, one may anticipate an upper bound for Δ_c of about 4 since w_e for large L coalesce onto a single curve for $\Delta \gtrsim 4$.

Finite-size scaling collapses of w_e can be used to determine Δ_c and ν . However we have shown²⁷ that more accurate values are obtained by examining the width of the interface dh along the direction z normal to the initial domain wall (x - y plane). We define dh as the distance between the highest and lowest points on the external interface, averaged over an ensemble of growth simulations for each cell size L . In the self-similar regime, the external interface is a fractal that spans the simulation cell and dh is expected to increase linearly with L . In the self-affine regime, $dh \sim L^H$, where H is called the Hurst or roughness exponent. As in earlier work,²⁰ we find H is consistent with $2/3$ for all Δ . Since $H < 1$, dh/L vanishes in the limit $L \rightarrow \infty$. Figure 3 shows dh/L vs Δ for $L=48$ to 768. As expected, all curves approach a constant at large Δ , and vanish as Δ decreases. The transition between limiting behaviors becomes narrower as L increases. The value of Δ_c can be identified with the point where all curves cross. As shown in Fig. 1, Δ_c lies near a local maximum in $H_c(\Delta)$. It is interesting to note that Δ_c is also at (or close to) a local maximum of H_c for the case of a Gaussian distribution of random fields.²⁷

A more quantitative analysis of the critical behavior was performed using finite-size scaling. The deviation from Δ_c is measured by $\delta \equiv (\Delta - \Delta_c)/\Delta$. For small δ , we assume that the only relevant lengths are $\xi \sim \delta^{-\nu}$ and the system size L . In this case, dh/L can only depend on L/ξ or, equivalently, on $L^{1/\nu}\delta$. This is confirmed by the data collapse shown in the inset of Fig. 3. We find acceptable collapses for $\Delta_c = 3.88 \pm 0.03$ and $\nu = 2.4 \pm 0.4$. We note that the value of ν is in complete agreement with the exponent obtained for a Gaussian distribution of random fields, indicating that the distribution of fields does not change the universality class.²⁷

B. Self-affine to faceted transition

Previous studies of the RFIM (Refs. 17–21) always show a crossover to a faceted regime at low disorder when the

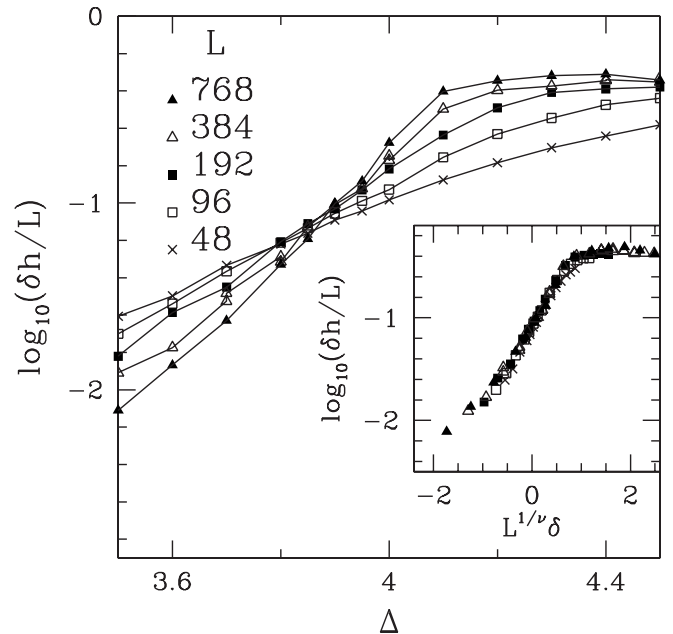


FIG. 3. Average height difference between top and bottom of external interfaces ($dh = \langle h_t - h_b \rangle$), normalized by system size L , as a function of disorder. The inset shows a finite-size scaling collapse of the data points when plotted versus $L^{1/\nu}\delta$, with $\nu=2.4$, $\delta=(\Delta - \Delta_c)/\Delta$ and $\Delta_c=3.88$.

distribution of random local fields is bounded. The faceted regime is removed for unbounded distributions, such as Gaussian disorder.²⁷ In 2D, there is a direct transition between faceted and self-similar growth for bounded disorder.¹⁷ The transition occurs at a unique value of disorder but the critical field at lower Δ depends on the boundary conditions and orientation of the initial interface.¹⁷ Boundary conditions and crystallographic orientation have more dramatic effects on the phase diagram for 3D systems shown in Fig. 1.

For $\Delta_0 < \Delta < \Delta_c$, we find self-affine growth for any geometry, and H_c is independent of geometry in the limit of infinite system size. Amaral *et al.*⁹ contrasted growth in this range of Δ to front propagation in models with intrinsic anisotropy in the equations of motion, such as the Kardar-Parisi-Zhang (KPZ) model.^{5,22} Intrinsic anisotropy led to a continuous variation in H_c with the angle of the initial interface relative to the crystallographic axes while no variation was observed for the 3D RFIM considered here. Earlier work by Ji and Robbins²⁰ had also concluded that there was no lattice anisotropy in the self-affine growth for $\Delta_0 < \Delta < \Delta_c$ in the 3D RFIM.

For $\Delta < \Delta_0$, lattice anisotropy becomes important. As shown in Fig. 1, we find that H_c depends on the interface orientation and boundary condition. However, in contrast to models with intrinsic anisotropy,^{9,10} H_c changes discontinuously with interface orientation. Following Amaral *et al.*,⁹ we considered periodic systems with interfaces oriented perpendicular to the (10λ) direction for λ equal to integers from 1 to 64. Finite-size scaling results gave the same $H_c(\Delta)$ (within 0.1%) for all values of λ (filled squares in Fig. 1), although the approach to the infinite-size limit was slower as λ in-

creased. The limit $\lambda \rightarrow \infty$ corresponds to the (001) orientation, and there is a discontinuous jump in H_c in this limit. Simulations for the (001) orientation show $H_c=4-\Delta$ which separates from the value of H_c for all other λ as Δ decreases below Δ_0 . Note that our results for H_c at all finite λ are also consistent with results for the (111) orientation performed for this paper and presented previously.²¹ For any direction other than (001), the interface eventually develops overhangs where the height is not single valued. These large deviations from the nominal growth direction restore isotropy in the depinning field. They become rarer as the direction approaches (001), and simulations with larger L are needed to determine H_c .

The emergence of a singular direction below Δ_0 might signal a new universality class with a different roughness exponent. To test the scaling, we studied the interface morphology for system sizes up to $L=3072$ and different orientations. When the growth direction is at a large angle from (001), scaling shows a roughness exponent of $2/3$, with an uncertainty of less than 0.02. While this exponent is the same as for $\Delta > \Delta_0$, the prefactor of the roughness becomes anisotropic for $\Delta < \Delta_0$.

We define the anisotropy in the roughness at a given scale ℓ by the ratio $R(\ell)$ of the root mean squared (rms) roughness along x and y directions. The rms roughness $h_i(\ell)$ along each direction $i=x, y$ is obtained by finding the rms height fluctuation along line segments of length ℓ along the desired direction. For a self-affine surface $h_i(\ell) \propto \ell^H$, where H is the Hurst or roughness exponent.^{1,2} Note that $R(\ell)$ must be unity for growth along symmetry directions with threefold or fourfold symmetry. We find $R(\ell)=1$ and $H=2/3$ for growth along the (111) direction, which is consistent with studies using anisotropic boundary conditions.²¹ As noted above, the fourfold symmetry direction (001) is a singular direction with a higher H_c and faceted morphology.

To study the variation in $R(\ell)$ with angle relative to the (001) direction, we considered growth from interfaces oriented perpendicular to the (10λ) direction. For $\Delta_0 < \Delta < \Delta_c$, $R(\ell)$ is equal to unity within statistical fluctuations of a few percent for all λ . Deviations from unity are apparent when Δ decreases below Δ_0 . For small λ , the value of $R(\ell)$ is nearly independent of ℓ . Figure 4 shows results for growth along (102) and (104) at $\Delta=1.7$. Note that the scaling along both x and y is consistent with $H=2/3$. The value of $R(\ell)$ approaches a constant at large ℓ (although fluctuations become significant near the system size). The length at which $R(\ell)$ saturates increases with λ , as the orientation approaches the singular (001) direction. This makes it increasingly difficult to obtain accurate exponents and apparent exponents that are slightly smaller (by up to 0.1) are observed for $L \leq 3072$ and growth along $(1\ 0\ 64)$. However, our results support the existence of a constant H with direction-dependent lattice anisotropy for $1 < \Delta < \Delta_0$. The sensitivity to growth direction in this regime is also reflected in the sensitivity to boundary conditions.

The effect of orientation and boundary conditions can be illustrated by considering the stability of flat regions with different crystallographic orientations in the low disorder limit. For an interface spin s_i with n nearest neighbors, f of which are flipped (+1) and $n-f$ unflipped (-1), the contribution to the total energy [Eq. (1)] is

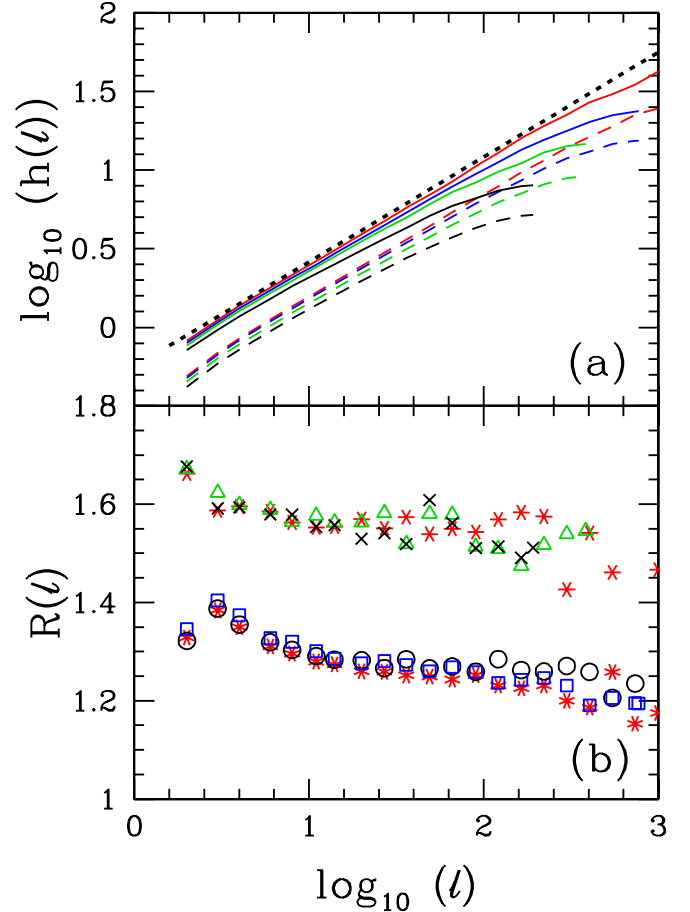


FIG. 4. (Color online) (a) Log-log plot of rms height fluctuation $h_i(\ell)$ over length ℓ along the $i=x$ (solid lines) and y (dashed lines) directions for $L=192, 384, 768,$ and 1536 in order of increasing height. The straight dotted line shows power law scaling with $H=2/3$. Here $\Delta=1.7$, and the initial interface is normal to the (102) direction. (b) Ratio $R(\ell)=h_x(\ell)/h_y(\ell)$ vs $\log_{10}(\ell)$ for growth orientations of (102) and (104) with $L=3072$ (circles), 1536 (asterisks), 768 (squares), 384 (triangles), and 192 (crosses). At large $\log_{10}(\ell)$, results for (102) saturate around 1.55 and results for (104) saturate near 1.25. In general, for growth along (10λ) , $R(\ell)$ approaches a constant at larger ℓ as λ increases.

$$\varepsilon_i = s_i(n - 2f - H - \eta_i). \quad (2)$$

The lowest external field that will cause such a spin to flip ($s_i=-1 \rightarrow s_i=+1$) is $H_i=n-2f-\eta_i$. In the limit of large system size, interface spins will sample all values of η_i . Since the distribution is bounded, the first spin will flip at $H_{min}=n-2f-\Delta$ and all spins will flip by $H_{max}=n-2f+\Delta$.

Consider first a (001) interface with periodic boundary conditions. Since $n=6$ and $f=1$, no spins will flip for $H < H_{min}=4-\Delta$. When H is increased enough to flip the first spin, its neighbors will have $f=2$. All of these neighbors will flip for $H > H_{max}=2+\Delta$ and they will cause all their neighbors to flip in turn. This chain reaction implies that $H_c=4-\Delta$ for $\Delta < 1$. The situation is more subtle for larger Δ , but $H_c=4-\Delta$ up to $\Delta_0 \approx 2.42$. As discussed in Ref. 20, the problem of flipping each plane can be mapped to bootstrap percolation on a two-dimensional square lattice and any flipped

spins are enough to produce percolation of flipped spins in the thermodynamic limit.

Introducing free boundary conditions reduces H_c (upper dashed line in Fig. 1) because spins at the boundary of the simulation cell have fewer neighbors and are easier to flip. Edge sites at the line where the interface hits the face of the cubic simulation cell have $n=5$ and $f=1$. Corner sites where the interface hits the edge of the simulation cell have $n=4$ and $f=1$. An upper bound for H_c is given by $2+\Delta$. At this field all corner spins flip. Their neighboring edge spins also flip since they have $f=2$ and $H_{max}=1+\Delta$. This sets off a chain reaction that fills the entire edge. All spins adjacent to the edge then flip since they have $n=6$, $f=2$, and $H_{max}=2+\Delta$. For $\Delta > 1/2$, a new mechanism reduces H_c . The first edge spins flip at $H_{min}=3-\Delta$, which is lower than the field required to flip all corners. This sets off a chain reaction filling all edge sites for $H > H_{max}=1+\Delta$. The internal spins next to the corners then have $f=3$ and will flip since $H > H_{max}=\Delta$. Their two neighbors then have $f=3$ and a chain reaction flips all spins adjacent to the edge. Spins flip line by line until the whole layer is flipped. This argument breaks down for $\Delta > 1$ where the chain reaction along edge sites may be broken by unfavorable random fields. However, we find $H_c=3-\Delta$ to larger Δ because, as for periodic boundary conditions, percolation occurs even when some spins do not flip immediately.

In some physical systems, the distribution of random fields may be different at the edge of a sample. One limiting case would be for the boundary to favor flipped spins $\eta_i = \Delta$. This does not change the arguments for the critical field given above. In the opposite limit $\eta_i = -\Delta$, none of the edge sites can flip before all the corners flip. We find $H_c=2+\Delta$ until the first internal spins flip. Then there is a crossover to the critical field for periodic boundary conditions $H_c=4-\Delta$ at $\Delta=1$. This line is not shown in Fig. 1.

Interface spins on (111) surfaces start with $n=6$ and $f=3$. The case of (anti)periodic boundary conditions is considered in Ref. 21. All interface spins flip for $H > H_{max}=\Delta$, giving an upper bound for H_c . For $\Delta > 1$, H_c drops below this upper bound. It is no longer necessary for all spins in a layer to flip immediately because some spins in the subsequent layer with $f=2$ can flip for $H > H_{min}=2-\Delta$. This will cause underlying spins to have $f=4$ and they will flip below $H=\Delta$. The result is a crossover to self-affine growth at $\Delta=1$.

In contrast to the (001) case, free boundary conditions increase H_c for (111) interfaces. For the initial interface, sites at the corners of the interface have $n=3$ and $f=1$, and edge sites have $n=4$ and $f=1$. While the internal spins all flip for $H > \Delta$, the edge and corner sites require higher fields. For $\Delta < H < H_c$ each successive layer of flipped spins covers a smaller area and the final pinned configuration contains a set of facets with (001) orientation. A typical example is shown for $H=1.1$ and $\Delta=0.25$ in Fig. 5.

As for the (001) orientation, an upper bound for H_c is provided by the field required to flip all corner sites $H_{max}=1+\Delta$. This allows adjacent edge sites to flip until the entire plane is filled. For $H < 2-\Delta$, edge sites can flip before all corner sites flip. This also nucleates a chain reaction and reduces H_c to $2-\Delta$ for $\Delta > 0.5$. The complete curve for H_c is indicated by the lower dashed line in Fig. 1.

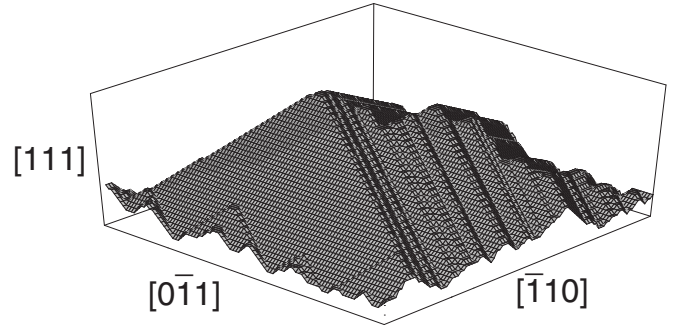


FIG. 5. Equilibrium pinned interface for a particular realization of growth with disorder $\Delta=0.25$ with initial interface along (111) plane and free boundary conditions (faceted regime). The external field, $H=1.1$, is smaller than $H_c(\Delta)$ in this case (see Fig. 1). Note that pinning is essentially due to the large $\langle 001 \rangle$ facets, which are the hardest to advance at low disorder.

C. Effect of boundaries on interface morphology

In terms of physical realization, only free boundary conditions are accessible to experiments since any sample is finite. Periodic or antiperiodic²¹ boundary conditions are frequently used in simulations because of convenience and the belief that they represent the limiting behavior of large systems most efficiently. The faceted growth regime represents an interesting case where growth phenomena are sensitive to boundaries—even in the $L \rightarrow \infty$ limit. Faceted growth is very sensitive to the easiest or most difficult spin to flip, which may often be on the boundary. Indeed, all results for $H_c(\Delta)$ in the faceted growth fall on straight lines given by

$$H_c(\Delta) = n - 2f \pm \Delta, \quad (3)$$

where the minus sign arises when the first spin to flip causes a chain reaction while the plus sign arises when the most difficult spin to flip can prevent the interface from advancing.

The impact of the intriguing variety of faceted growth regimes shown in Fig. 1 on interfaces in finite systems is illustrated in Fig. 5. This system had an initial (111) interface at the bottom of a diamond-shaped prism with free boundary conditions. The prism was cut from the crystal with 60° angles at the left and right corners and 120° angles at the front and back. A relatively small simulation cell, with $L=100$ spins on each edge, was taken for the qualitative discussion here.

Figure 5 shows a pinned interface at $H=1.1$ and $\Delta=0.25$. Little additional growth occurs until the field is close to the critical field of $H_c(0.25)=1.25$ for free boundaries. The asymmetry between the left and right halves of the system reflects the crystalline structure, which only has threefold symmetry about the base of the prism.

Note that the pinned interface has advanced relatively little near the boundaries. These represent the bottlenecks, where the interface cannot advance until all spins with $n-2f=1$ can flip. Spins in the central region see an environment close to that of a periodic system and flip when $H > \Delta$. This advance is halted near the edge, and a smaller area is able to advance with each successive layer. The final

pinned interface consists mainly of facets oriented along the hard (001) growth directions that hit the boundary near the initial height. These facets cannot advance until the much higher critical field of 2.25. Growth would be very different with periodic boundary conditions. For example, a periodic repetition of the interface in Fig. 5 would have sharp valleys at the boundaries between periodic images. The number of neighboring flipped spins at the bottom of these valleys is very high, causing them to fill in rapidly and allowing the entire interface to advance. Qualitatively similar behavior is found for other boundary shapes and initial interface orientations.

Figures 1 and 5 clearly show the strong effect of boundary conditions. While (111) is the easy growth direction for periodic boundary conditions, free boundary conditions cause the more difficult (100) facets to develop and remain pinned at the boundary. In contrast, free boundaries can assist faceted growth of interfaces with a (001) orientation, lowering H_c by as much as a factor of 2. Other effects on real boundaries, including roughness and changes in the distribution of disorder may lead to even more complex behavior.

IV. SUMMARY AND CONCLUSIONS

The results presented above reveal aspects of the rich phase diagram of interface growth in three-dimensional random field systems with bounded disorder. In addition to the self-similar and isotropic self-affine regimes observed for Gaussian disorder, there are anisotropic self-affine and faceted regimes at low disorder (Fig. 1). For weak disorder, growth is strongly affected by boundary conditions as well as crystalline anisotropy.

The critical field H_c needed to initiate steady motion and the morphology of the pinned interface at H_c were studied as a function of disorder Δ . The transition between self-similar interfaces at high disorder and self-affine morphology at intermediate disorder was studied using finite-size scaling. The transition occurs at a critical disorder of $\Delta_c = 3.88 \pm 0.03$ and the correlation diverges with an exponent $\nu = 2.4 \pm 0.4$. The value of ν is consistent with results for unbounded disorder, suggesting that bounds on the disorder do not affect the universality class of this transition. The transition also occurs near a local maximum in H_c for both bounded and unbounded disorder. One may expect that this is a consequence of the fact that disorder disrupts self-affine growth and thus increases H_c while disorder enhances percolative growth and thus lowers H_c . Note that disorder favors self-similar growth because the percolation probability is less than 1/2. In the limit of large disorder, the spins that flip have random fields below the mean of zero, and these fields become more negative as Δ increases.

The value of Δ_c is significantly different than an earlier estimate²⁰ of 3.41. This estimate was based on the scaling of a finger width w that we have shown (Fig. 2) does not diverge at Δ_c because of local patches of unflipped spins that are left behind the interface. As in earlier studies of unbounded disorder,²⁷ a finger width w_e derived from the external interface does diverge at Δ_c . Scaling studies of w_e give values of Δ_c and ν that are consistent with results from other

quantities, such as the ratio of interface width to system size (Fig. 3).

The above value for ν is substantially different from the value $\nu=1.4$ from RFIM models where noninterface spins can flip.^{14–16} A recent study by Liu and Dahmen¹⁶ found an even lower value of ν in this growth model when the random fields had the uniform distribution considered here. Their studies start with all spins initially down and can be viewed as yet another type of boundary condition for the front propagation model. The first spin will flip at $H=6-\Delta$, lowering the barrier for its neighbors to flip. In a sufficiently large system, the resulting clusters will be able to grow throughout the system if they are above the $H_c(\Delta)$ in Fig. 1. We find $6-\Delta$ equals $H_c(\Delta)$ near $\Delta=4.6$ which is consistent with the critical disorder found by Liu and Dahmen. It would be interesting to explore this connection between the models in more detail.

For intermediate disorder, $\Delta_0 < \Delta < \Delta_c$, we find growing interfaces are self-affine with roughness exponent $H=2/3$. As in previous studies,²⁰ the critical field is independent of the type of boundary conditions and of the crystallographic orientation of the initial interface. The growing interface is also isotropic, with the same change in height for different directions along the interface.

Below $\Delta_0=2.42$, H_c and the interface morphology become strongly dependent on the initial orientation and boundary conditions. For growth along (001) and periodic boundary conditions, the interface is a flat facet up to $H_c=4-\Delta$. All inequivalent growth directions have the same, lower value of H_c and the pinned interface is self-affine. While the interface has the same roughness exponent as was found above Δ_0 , the interface may be anisotropic. As shown in Fig. 4, height differences grow more rapidly with separation along one direction than along the perpendicular direction. This anisotropy vanishes by symmetry along the (111) direction, which is why it would not have been evident in studies with this orientation.²¹

Continuous changes in H_c with growth direction have been seen in other models where, unlike the RFIM, the interface height must be single valued.^{9,10} The discontinuous transition seen here seems more analogous to equilibrium roughening transitions.³⁰ In thermal roughening transitions, the total roughness of facets with a given orientation is finite below the transition temperature T_c . Above T_c , the roughness diverges with the facet size. By analogy to this transition, we can say that the disorder at which the (001) surface roughens is Δ_0 while all other orientations are above their roughening transition for $\Delta > 1$.

The possibility of a roughening transition in interfacial growth models has been considered analytically. The conclusion is that three-dimensional systems should only have a roughening transition when there are long-range power-law interactions.³¹ However, these studies used models that explicitly break symmetry by assuming that the interface height is a single-valued function of position and expressing the interfacial energy as the squared gradient of height. Other predictions for such models are also very different than for the RFIM. For example, there is no self-similar regime in such models and the interface can be stopped by a single insurmountable random field.^{20,27}

As Δ decreases below unity, growth along (111) is much easier than any other direction when there are periodic boundary conditions. Along this direction $H_c = \Delta$, while $H_c = 4 - \Delta$ for the (001) direction and $H_c = 2 - \Delta$ for all other directions. In all cases, the interface is faceted at the onset of growth. By analogy with the roughening transition, one might say that all orientations are below the roughening transition in this regime.

Periodic boundary conditions are not accessible to experiments and the interface morphology is very sensitive to boundary conditions at low disorder. Free boundary conditions ease growth along the (001) direction but inhibit growth along the (111) direction. For all but the (001) direction, $H_c = 2 - \Delta$ for $0.5 < \Delta < 1$. A range of H_c can be obtained if the interface enhances growth or inhibits growth. Both may be relevant in experimental systems.

While we considered spins on a simple cubic lattice, we expect that the sequence of transitions will be the same for any three-dimensional lattice. This was generally true in the case of two-dimensional systems studied earlier, with the exception of the honeycomb lattice because of its low coordination number.^{17,18} It would be interesting to see if the low

coordination number of the diamond lattice led to any changes in behavior at low disorder.

Recent experiments reporting propagation of domain walls in magnetic nanowires³² show that magnetization reversal under an external magnetic field and the domain-wall velocity are now accessible to control and may be employed in applications such as magnetoelectronic devices. In spite of the simplicity of the model (RFIM) discussed in this paper, we expect that the sample preparation, involving the degree of disorder and the crystallographic growth orientation, are key physical aspects to be explored in tailoring properties (such as switching times) for specific applications.

ACKNOWLEDGMENTS

We thank Colin Denniston for assistance in the preparation of Fig. 5 and Karin Dahmen for useful discussions. This material is based on work supported by the National Science Foundation under Grant No. DMR 0454947. B.K. acknowledges financial support from CNPq, FAPERJ, FUJB, and Millenium Institute of Nanotechnology-MCT in Brazil.

-
- ¹F. Family and T. Vicsek, *Dynamics of Fractal Surfaces* (World Scientific, Singapore, 1991).
- ²A.-L. Barabási and H. E. Stanley, *Fractal Concepts in Surface Growth* (Cambridge, Cambridge, England, 1995).
- ³G. Ódor, *Rev. Mod. Phys.* **76**, 663 (2004).
- ⁴J. P. Sethna, K. A. Dahmen, and C. R. Myers, *Nature (London)* **410**, 242 (2001).
- ⁵M. Kardar, G. Parisi, and Y.-C. Zhang, *Phys. Rev. Lett.* **56**, 889 (1986).
- ⁶O. Narayan and D. S. Fisher, *Phys. Rev. B* **48**, 7030 (1993).
- ⁷P. Le Doussal, K. J. Wiese, and P. Chauve, *Phys. Rev. B* **66**, 174201 (2002); A. B. Kolton, G. Schehr, and P. Le Doussal, *Phys. Rev. Lett.* **103**, 160602 (2009).
- ⁸A. Rosso, P. Le Doussal, and K. J. Wiese, *Phys. Rev. B* **80**, 144204 (2009).
- ⁹L. A. N. Amaral, A.-L. Barabási, and H. E. Stanley, *Phys. Rev. Lett.* **73**, 62 (1994).
- ¹⁰L.-H. Tang, M. Kardar, and D. Dhar, *Phys. Rev. Lett.* **74**, 920 (1995).
- ¹¹H. Leschhorn, T. Nattermann, S. Stepanow, and L.-H. Tang, *Ann. Phys.* **509**, 1 (1997).
- ¹²F.-J. Pérez-Reche, L. Truskinovsky, and G. Zanzotto, *Phys. Rev. Lett.* **101**, 230601 (2008).
- ¹³G. Durin and S. Zapperi, in *The Science of Hysteresis*, edited by G. Bertotti and I. Mayergoy (Academic, New York, 2005), pp. 181–267.
- ¹⁴O. Perković, K. Dahmen, and J. P. Sethna, *Phys. Rev. Lett.* **75**, 4528 (1995).
- ¹⁵O. Perković, K. A. Dahmen, and J. P. Sethna, *Phys. Rev. B* **59**, 6106 (1999).
- ¹⁶Y. Liu and K. A. Dahmen, *Phys. Rev. E* **79**, 061124 (2009).
- ¹⁷H. Ji and M. O. Robbins, *Phys. Rev. A* **44**, 2538 (1991).
- ¹⁸B. Koiller, H. Ji, and M. O. Robbins, *Phys. Rev. B* **46**, 5258 (1992).
- ¹⁹U. Nowak and K. D. Usadel, *Europhys. Lett.* **44**, 634 (1998).
- ²⁰H. Ji and M. O. Robbins, *Phys. Rev. B* **46**, 14519 (1992).
- ²¹L. Roters, A. Hucht, S. Lubeck, U. Nowak, and K. D. Usadel, *Phys. Rev. E* **60**, 5202 (1999).
- ²²The KPZ and related models break rotational symmetry by identifying a specific growth direction and requiring the interface to be single valued along this axis. In the RFIM model, the external field always drives growth perpendicular to the local interface orientation even if that evolves over time.
- ²³J. P. Stokes, A. P. Kushnick, and M. O. Robbins, *Phys. Rev. Lett.* **60**, 1386 (1988).
- ²⁴M. Cieplak and M. O. Robbins, *Phys. Rev. Lett.* **60**, 2042 (1988); *Phys. Rev. B* **41**, 11508 (1990).
- ²⁵M. Bahiana, B. Koiller, S. L. A. de Queiroz, J. C. Denardin, and R. L. Sommer, *Phys. Rev. E* **59**, 3884 (1999).
- ²⁶P. Bak, C. Tang, and K. Wiesenfeld, *Phys. Rev. A* **38**, 364 (1988).
- ²⁷B. Koiller and M. O. Robbins, *Phys. Rev. B* **62**, 5771 (2000).
- ²⁸This is close to the value of P at H_c in finite-size scaling studies. See Figs. 1 and 2 of Ref. 27.
- ²⁹N. Martys, M. Cieplak, and M. O. Robbins, *Phys. Rev. Lett.* **66**, 1058 (1991); N. Martys, M. O. Robbins, and M. Cieplak, *Phys. Rev. B* **44**, 12294 (1991).
- ³⁰H. van Beijeren, *Phys. Rev. Lett.* **38**, 993 (1977); V. J. Emery and R. H. Swendsen, *ibid.* **39**, 1414 (1977).
- ³¹T. Emig and T. Nattermann, *Phys. Rev. Lett.* **81**, 1469 (1998), and references therein.
- ³²T. Ono, H. Miyajima, K. Sigeto, K. Mibu, N. Hosoito, and T. Shinjo, *Science* **284**, 468 (1999).